Periodico di Mineralogia (2014), 83, 2, 241-255 DOI: 10.2451/2014PM0014

PERIODICO di MINERALOGIA
established in 1930

An International Journal of
MINERALOGY, CRYSTALLOGRAPHY, GEOCHEMISTRY,
ORE DEPOSITS, PETROLOGY, VOLCANOLOGY
and applied topics on Environment, Archaeometry and Cultural Heritage

Oxidation degree of chromite from Indian ophiolites: a crystal chemical and ^{57}Fe Mössbauer study

Davide Lenaz[1,*], Giovanni B. Andreozzi[2], Maibam Bidyananda[3]
and Francesco Princivalle[1]

[1]Dipartimento di Matematica e Geoscienze, Università di Trieste, Via Weiss 2 - 34127 Trieste, Italy
[2]Dipartimento di Scienze della Terra, Sapienza Università di Roma, Piazzale A. Moro 5 - 00185 Roma, Italy
[3]Department of Earth Sciences, Manipur University, Canchipur, Imphal-795003 India
[*]Corresponding author: *lenaz@units.it*

Abstract

Several samples of Cr-bearing spinel from Indian ophiolites have been studied by X-ray single crystal diffraction and structure refinement, electron probe microanalyses and Mössbauer spectroscopy. Differences between samples coming from massive chromitite bands and those coming from podiform chromitite deposits have been evidenced: the former have (Mg,Fe)-chromite component ≥ 75%, the latter from 69 to 74%. In both cases the complementary components are aluminate (mainly spinel sensu stricto $MgAl_2O_4$). As magnesiochromite ($MgCr_2O_4$) is always dominant with respect to chromite ($FeCr_2O_4$), the studied samples are classified as magnesiochromite. The multi-analytical approach has revealed that some of the studied spinels are non-stoichiometric (due to Fe^{2+} oxidation and vacancy formation), with those coming from massive chromitite being more oxidised than those from the pods. Comparison between our results and recent literature suggested that spinel oxidation is more common than usually believed: it is not restricted to ophiolites but may occur in different geological settings and may help reconstructing the complex thermo-oxidative history of the host rock. Consequently, the proposed multi-analytical approach is crucial for an accurate crystal chemical characterisation of spinels and other Fe-bearing mineral phases, especially when geothermobarometric calculations have to be performed.

Key words: chromite; single crystal X-ray diffraction; Mössbauer spectroscopy; non-stoichiometry; oxidation.

Introduction

Chromite and magnesiochromite are minerals belonging to the spinel group with $FeCr_2O_4$ and $MgCr_2O_4$ chemical formula, respectively, and $Fd\bar{3}m$ cubic symmetry. They are not only useful indicators of crystallisation environment, but also reliable recorders of modifications induced during early hydrous alteration and subsequent prograde metamorphism of host rocks. There are several studies regarding "chromite" (including magnesiochromite) chemical alterations during metamorphic modification of ultramafic complexes (Ulmer, 1974; Evans and Frost, 1975; Kimball, 1990; Burkhard, 1993; Barnes, 2000). Chromite crystal first becomes rimmed and progressively replaced by chromian magnetite (or "ferritchromit"); successively its core composition becomes progressively modified during prograde metamorphism as a result of chemical exchange with the surrounding silicates. The most common chemical reactions are Mg substitution by Fe^{2+} and then Fe^{2+} oxidation to Fe^{3+}.

The oxidation state of ferrian spinels may be evaluated by measuring maghemitization and the (possible) subsequent martitization of the samples. The two processes are closely interconnected, as maghemitization involves the transformation of Fe^{2+} to Fe^{3+} and martitization the exsolution of α-Fe_2O_3. Both processes are related to trivalent-for-divalent cation substitution at the spinel T site and a decrease in the *u* oxygen positional parameter of the spinel structure. The former effect modifies Fe^{2+} and Fe^{3+} contents and may be evaluated either by stoichiometry via electron probe microanalysis (EPMA) or experimentally via ^{57}Fe Mössbauer spectroscopy (MS), which obviously discriminates the Fe^{2+} and Fe^{3+} better than EPMA (Mitra et al., 1991a, 1991b; Carbonin et al., 1996; Li et al., 2002; Quintiliani, 2005; Quintiliani et al., 2006; Lenaz et al. 2013). The latter can be easily determined by X-ray single crystal diffraction and structure refinement (SREF) in combination with EPMA (Menegazzo et al., 1997; Menegazzo and Carbonin, 1998; Carbonin et al., 1999; Lenaz et al., 2002, 2009; Derbyshire et al., 2013). However, the two approaches have been rarely combined (Carbonin et al., 1996; Bosi et al., 2004; Lenaz et al., 2004, 2014b; Perinelli et al., 2014).

In this work selected chromite samples from two ophiolite belts of India, Indus-Tsangpo Suture Zone and the Indo-Myanmar Range, have been investigated by means of SREF, EPMA and MS. The aim of this study is the determination of chromite oxidation degree, to help reconstruction of their thermal path and oxidation history.

Geological setting

India collided with the southern margin of Eurasia in early Cenozoic time along the Indus-Tsangpo Suture Zone (Figure 1). The suture along the Indus-Tsangpo river in the Himalaya continues southward along Indo-Myanmar Hill Ranges, Andaman and Nicobar Islands in Bay of Bengal to Indonesian trench. Along the suture fragments of oceanic lithosphere have been preserved as obducted ophiolitic bodies, forming a discontinuous belt. Three ophiolite occurrences are known in India, the Indus Suture Ophiolite

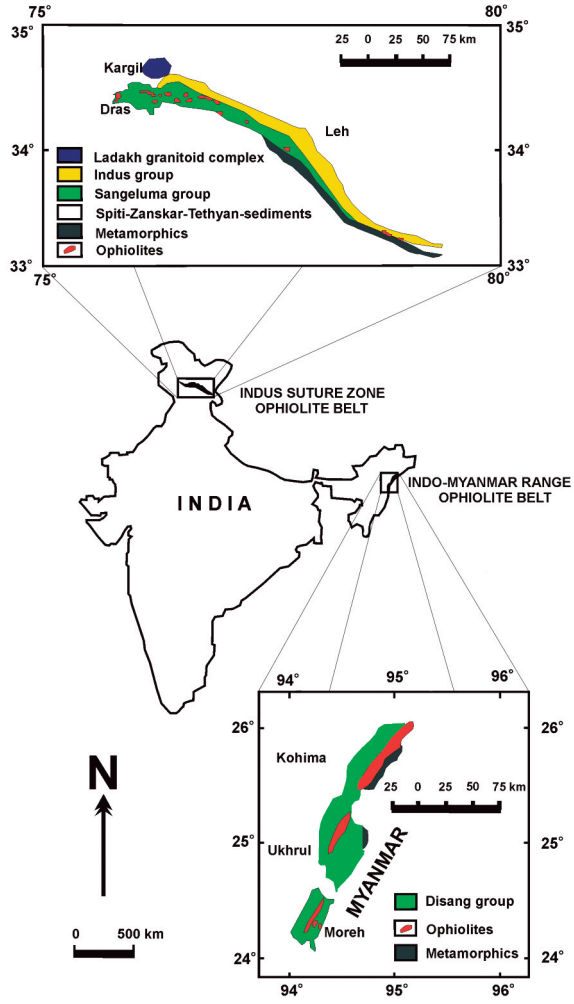

Figure 1. Map showing the studied ophiolite belts (modified after Prasad, 1984).

belt, the Indo-Myanmar Ranges and the Andaman and Nicobar Islands, but only the first two will be described as they host the chromite samples studied in this work.

The Indus Suture zone at Ladakh, northwestern Himalayas lies between the Tethys Himalaya Zone of Spiti and Zanskar in the south and the Karakoram in the north. It is characterized by the presence of ophiolitic sequences, mélanges, plutonic-volcanic association of magmatic arc, flysch and molasses (Thakur, 1981). Among the many ophiolite belts in the region, a complete ophiolitic sequence is exposed in the Nidar area in the Eastern Ladakh. It comprises ultramafites,

gabbro, diorites, pillow lavas and radiolarian chert. Chromite occurs in massive chromitite bands (1 m thick bodies in ultramafic rocks) and as disseminated grains. Samples RN31 and RN33 are representative of the massive chromitite bands.

The ophiolite belt of the Indo-Myanmar Ranges is exposed as steeply inclined narrow sheets, ranging from a few kilometres to tens of kilometres in length. The ophiolite belt occurring along the Indo-Myanmar border extends for about 200 km from Chiphur (Nagaland state) in the north to Moreh (Manipur state) in the south with an average width of 15 km. The belt comprises dunite, peridotite, pyroxenite, gabbro, mafic volcanics and associated oceanic pelagic sediments. In the area chromite occurs in podiform chromitite deposits (1 m x 3 m), in nodules, and as disseminated grains within the ultramafites. Samples GAM1, GAM3, N-17A, N21 and N21A are representative of the podiform chromitite deposits (hereafter called pods).

Experimental

Single crystal X-ray diffraction

Nine chromite single crystals from several samples of chromitite have been selected and analysed by SREF. X-ray diffraction data were recorded on an automated KUMA-KM4 (K-geometry) diffractometer, using MoKα radiation, monochromatised by a flat graphite crystal, at the University of Trieste (Italy). Data collection was made, according to Della Giusta et al. (1996), up to 55° of 2θ in the ω-2θ scan mode, scan width 1.8° 2θ, counting time 20-50 seconds. Twenty-four equivalent reflections of (12 8 4) peak, at about 80° of 2θ, were accurately centred at both sides of 2θ, and the α_1 peak barycentre was used for cell parameter determination. Corrections for absorption were performed according to North et al. (1968). Structural refinement using the SHELX-97 program (Sheldrick, 2008) was carried out against Fo^2_{hkl} in the *Fd$\bar{3}$m space* group (with origin at *$\bar{3}$m*), since no evidence of different symmetry appeared. Refined parameters were scale factor, oxygen positional parameter (*u*), tetrahedral and octahedral site occupancies and thermal displacement parameter (U). Scattering factors were taken from Prince (2004) and Tokonami (1965). No constraints were imposed by chemical analyses. Crystallographic data are listed in Table 1.

Electron Probe MicroAnalyses

Two of the nine crystals studied by SREF were unfortunately lost during subsequent preparation for EPMA. On the seven crystals remaining, the same used for X-ray data collection, ten to fifteen chemical spot analyses were collected using a CAMECA SX50 electron microprobe at the CNR laboratory in Padova, operated at 15 kV and 15 nA, 10 s counting time for peak and 5 sec for total background. Synthetic oxide standards (MgO, Fe_2O_3, MnO, ZnO, NiO, Al_2O_3, Cr_2O_3, TiO_2 and SiO_2) were used. Raw data were reduced with PAP-type correction software provided by CAMECA. Results are considered accurate between 2-3% for major elements and 10% for minor elements. As usual, iron was expressed as ferrous oxide, and, as a first step, ferric iron was calculated by stoichiometry (Table 2).

Table 1. Results of structure refinement of chromite samples from Indian ophiolites.

	GAM1	GAM3	N-17A	N21	N21A	RN31	RN33
a	8.2889(3)	8.2855(4)	8.2886(4)	8.2865(3)	8.2900(1)	8.3027(3)	8.3023(3)
u	0.26230(9)	0.26224(10)	0.26213(9)	0.26222(6)	0.26221(8)	0.26194(11)	0.26204(6)
T-O	1.971 (1)	1.969 (1)	1.969 (1)	1.9693 (9)	1.970 (1)	1.9693 (9)	1.971 (1)
M-O	1.9755 (7)	1.9751 (8)	1.9767 (7)	1.9756 (5)	1.9765 (6)	1.9815 (8)	1.9807 (8)
m.a.n.T	15.8 (1)	15.6 (2)	16.20 (9)	16.0 (2)	16.1 (2)	15.9 (2)	16.2 (1)
m.a.n.M	21.3 (2)	21.1 (4)	21.3 (2)	21.1 (4)	21.4 (4)	22.0 (4)	22.0 (2)
$m.a.n._{X\text{-}ray}$	58.4 (6)	57.9 (9)	58.9 (4)	58.1 (9)	58.9 (9)	60.0 (9)	60.2 (5)
$m.a.n._{chem}$	58.4	58.3	58.9	58.7	58.8	59.9	60.1
N_{refl}	175	158	173	187	167	170	176
U (M)	751 (9)	357 (10)	667 (8)	375 (8)	362 (9)	479 (12)	399 (6)
U (T)	939 (18)	523 (25)	857 (14)	580 (17)	569 (21)	654 (28)	606 (15)
U (O)	932 (20)	552 (26)	840 (18)	589 (17)	532 (22)	618 (25)	561 (15)
R1	2.23	2.67	1.94	2.04	2.22	3.43	1.77
wR2	5.19	4.9	3.93	3.85	4.38	6.55	3.45
GooF	0.785	1.352	0.898	1.362	1.322	1.192	1.223

*Note*s: *a* = cell parameter (Å); *u* = oxygen positional parameter; T-O and M-O = tetrahedral and octahedral bond lenghts (Å), respectively; m.a.n.T and m.a.nM = mean atomic number of T and M sites; $m.a.n._{X\text{-}ray}$ and $m.a.n._{chem}$ = mean atomic number calculated via X-ray refinement and electron microprobe; U(M), U(T), U(O) = displacement parameters for M site, T site and O; N. Refl. = number of unique reflections; R1 all (%), wR2 (%), GooF as defined in Sheldrick (2008). Estimated standard deviations in brackets.

Table 2. Average chemical composition of chromite samples from Indian ophiolites.

	GAM1	GAM3	N-17A	N21	N21A	RN31	RN33
MgO	15.4 (3)	15.48 (9)	14.7 (3)	14.8 (2)	14.9 (2)	14.9 (1)	14.4 (2)
Al_2O_3	13.9 (14)	14.2 (1)	13.3 (2)	13.5 (1)	13.2 (2)	10.2 (1)	10.18 (8)
SiO_2	0.12 (4)	0.12 (3)	0.16 (3)	0.12 (3)	0.12 (3)	0.12 (5)	0.13 (2)
TiO_2	0.20 (2)	0.19 (4)	0.19 (5)	0.22 (3)	0.25 (2)	0.17 (4)	0.20 (3)
Cr_2O_3	55.5 (6)	55.5 (1.0)	57.1 (6)	57.6 (3)	57.4 (3)	60.5 (7)	60.7 (6)
MnO	0.20 (6)	0.22 (5)	0.21 (6)	0.20 (5)	0.19 (7)	0.20 (4)	0.22 (3)
FeO_{tot}	13.7 (2)	14.0 (3)	13.4 (2)	12.9 (3)	13.0 (3)	13.4 (3)	13.0 (4)
NiO	0.16 (7)	0.16 (7)	0.14 (5)	0.14 (3)	0.14 (6)	0.00	0.16 (2)
Sum	99.19	99.82	99.18	99.44	99.07	99.48	99.02
FeO	10.5	10.5	11.5	11.4	11.2	10.9	11.3
Fe_2O_3	3.60	3.9	2.11	1.6	2.0	2.8	1.9
Sum	99.55	100.33	99.39	99.60	99.27	99.76	99.21

Notes: 10 to 15 spot analyses for each crystal. FeO and Fe_2O_3 calculated according to spinel stoichiometry. Average standard deviation in brackets.

^{57}Fe Mössbauer spectroscopy

The ^{57}Fe Mössbauer spectra were collected on samples RN31 and N21, representative of massive chromitite and pods, respectively. Mössbauer absorbers were prepared by pressing finely ground spinel samples mixed with powdered acrylic resin (Lucite) to self-supporting discs. The amount used corresponded to about 2 mg Fe/cm^2 and was well below an absorber density where thickness affects the Mössbauer results. Spectra were collected at 298 K (room temperature, *RT*) using a conventional spectrometer system operating in constant acceleration mode with a ^{57}Co source in rhodium matrix. Spectral data for the velocity range -4 to +4 mm/s were recorded in a multichannel analyser using 512 channels. After velocity calibration with a high purity α-iron foil spectra, the raw data were folded to 256 channels. The spectra were fitted using the Recoil 1.04 (Lagarec and Rancourt, 1998) fitting program and assuming symmetrical Lorentzian peak shapes. The best fits were evaluated by reduced χ^2, and uncertainties were calculated using the covariance matrix. Estimated errors are ±0.02 mm/s for centre shift (CS), quadrupole splitting (QS) and peak full width at half maximum (FWHM), and no less than ±3% absolute for absorption areas (A).

Mössbauer spectra of the two samples are dominated by a broad absorption band with CS close to 1 mm/s and QS values variable between 0.6 and 1.7 mm/s (Figure 2). In agreement with the existing literature (e.g., Hålenius et al., 2002; Bosi et al., 2004; Lenaz et al., 2004; Quintiliani et al., 2006; Adetunji et al., 2013), this part of the absorption envelope is considered to be due to ferrous iron. The observed broad absorption is a typical feature, because in the spinel structure Fe^{2+} mainly populates the tetrahedrally-coordinated T site, which is surrounded by 12 octahedrally-coordinated M sites; therefore, a broad absorption of Fe^{2+} doublets can be expected due to heterogeneous cation population at the M sites. An additional band is also present in the central part of the absorption spectrum with CS close to 0.3 mm/s, and this is commonly considered to be due to ferric iron. Several fitting strategies were tested

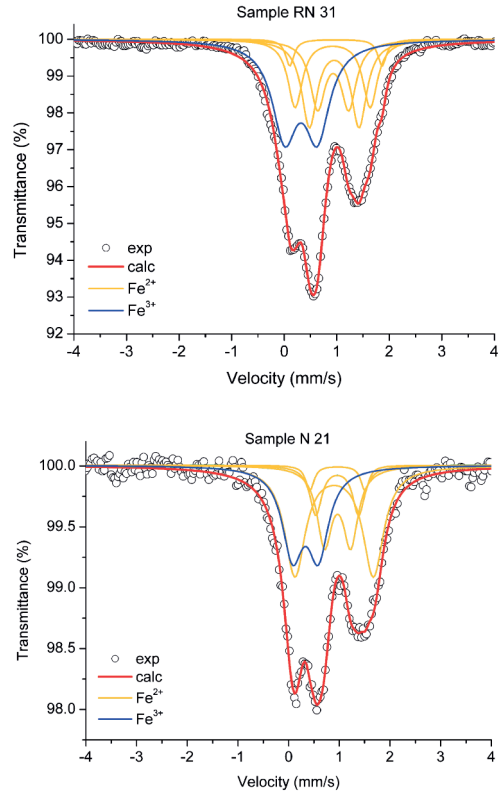

Figure 2. Room temperature ^{57}Fe Mössbauer spectra of Indian chromite samples RN31 and N21, representative of massive chromitite and pods, respectively.

to find a robust model that could be used with as few constraints as possible. The final model consisted of three outer doublets representing the broad contribution of tetrahedrally-coordinated Fe^{2+} (QS from 0.94 to 1.76 mm/s), one inner doublet for the contribution of octahedrally-coordinated Fe^{2+} (QS 0.57-0.59 mm/s), and one central doublet due to Fe^{3+}. To account for temperature effect, spectral areas measured for Fe^{2+} and Fe^{3+} at *RT* were corrected with the *f* factors calculated by De Grave and Van Alboom (1991): $f_{2+} = 0.687$ and $f_{3+} = 0.887$. The obtained doublet hyperfine parameters and absorption areas are listed in Table 3.

Table 3. ^{57}Fe Mössbauer hyperfine parameters of two representative chromite samples from Indian ophiolites.

Sample	CS (mm/s)	QS (mm/s)	FWHM (mm/s)	A (%)	Assignment
RN31	0.98	1.76	0.19	67	Fe^{2+}
	0.92	1.43	0.34		
	0.95	0.94	0.36		
	0.93	0.59	0.35		
	0.32	0.62	0.57	33	Fe^{3+}
N21	0.97	1.72	0.30	75	Fe^{2+}
	0.90	1.46	0.38		
	0.96	0.99	0.30		
	0.97	0.57	0.39		
	0.28	0.57	0.51	25	Fe^{3+}

Notes: Temperature = 298 K. CS = centre shift (with respect to α-iron foil); QS = quadrupole splitting; FWHM = full width at half maximum; A = absorption area, corrected for the temperature effect according to De Grave and Van Alboom (1991). Estimated uncertainties are about 0.02 mm/s for CS, QS and FWHM, and no less than 3% absolute for A.

Cation distribution

Cation distribution between T and M sites were obtained with the method described by Lavina et al. (2002), in which crystal chemical parameters are calculated as a function of the atomic fractions at the two sites and fitted to the observed ones. Site atomic fractions are calculated by minimising the function F(X) which takes into account the mean of the square differences between calculated and observed parameters, divided by their square standard deviations. Results of cation distribution for the studied samples are reported in Table 4.

Results and Discussion

Samples RN31 and RN33 coming from massive chromitite bands differ from the others coming from the pods mainly for the chromium content: these two samples, in fact, show Cr_2O_3 contents higher than 60 wt.% whereas the remaining samples show Cr_2O_3 lower than 58 wt.% (Table 2). In terms of crystal chemistry, samples RN31 and RN33 contain Cr close to (or higher than) 1.5 atoms per formula unit (apfu), which corresponds to a content of nominal (Mg,Fe)-chromite end member component ≥ 75%. The other samples show a nominal (Mg,Fe)-chromite component ranging from 69 to 74%. In both cases the complementary components are aluminate spinels, with spinel sensu stricto ($MgAl_2O_4$) prevailing on the others. For all samples magnesiochromite ($MgCr_2O_4$) component is dominant with respect to chromite ($FeCr_2O_4$), therefore, strictly speaking, the studied samples are magnesiochromite. In spite of

Table 4. Cation distribution of chromite samples from Indian ophiolites.

	GAM1	GAM3	N-17A	N21	N21A	RN31	RN33		$N21_{MS}$	$RN31_{MS}$
T site										
Mg	0.722	0.723	0.687	0.688	0.694	0.701	0.689		0.692	0.711
Al	0.003	0.004	0.007	0.009	0.008	0.000	0.013		0.006	0.006
Si	0.004	0.004	0.005	0.004	0.004	0.004	0.004		0.004	0.003
Mn	0.005	0.006	0.006	0.005	0.005	0.005	0.006		0.005	0.006
Fe^{2+}	0.246	0.226	0.258	0.260	0.259	0.247	0.260		0.254	0.227
Fe^{3+}	0.020	0.037	0.037	0.034	0.030	0.043	0.028		0.039	0.048
								Vac	0.000	0.000
M site										
Mg	0.001	0.004	0.007	0.008	0.010	0.009	0.003		0.004	0.002
Al	0.514	0.520	0.491	0.495	0.486	0.387	0.375		0.499	0.378
Ti	0.005	0.005	0.004	0.005	0.006	0.004	0.005		0.005	0.004
Cr	1.395	1.375	1.435	1.442	1.442	1.532	1.550		1.443	1.529
Fe^{2+}	0.031	0.042	0.046	0.042	0.035	0.043	0.046		0.044	0.043
Fe^{3+}	0.050	0.050	0.013	0.004	0.017	0.025	0.017		0.000	0.008
Ni	0.004	0.004	0.004	0.004	0.004	0.000	0.004		0.004	0.000
								Vac	0.002	0.019
F(X)	0.377	0.283	0.095	0.050	0.071	0.122	0.085	F(X)	0.095	0.160

Notes: $N21_{MS}$ and $RN31_{MS}$ = cation distribution for N21 and RN31 samples taking into consideration Mössbauer results. F(x) = minimisation factor, which takes into account the mean of square differences between calculated and observed parameters, divided by their standard deviations. Vac = vacancies.

this, the general name "chromite" will still be used hereafter because it is largely used in the geological community to identify Cr-rich spinels (see also Biagioni and Pasero, 2014).

On the basis of their (Mg,Fe)-chromite content and according to recent podiform chromitite classification revisited by Miura et al. (2012), Indian samples coming from the pods should belong to discordant podiform chromitite bodies, which involves precipitation from relatively hydrous melt and shallow magmatic origin. More generally, on the basis of oxygen positional

parameter and cell edge, various occurrence fields have been defined in the past for spinels (Figure 3). This was done through contributions of a number of studies, which identified the field for spinels coming from mantle xenoliths (Della Giusta et al., 1986, 1996; Princivalle et al., 1989; Carraro, 2003; Uchida et al., 2005; Nédli et al., 2008; Lenaz et al., 2014a; Perinelli et al., 2014; Princivalle et al., 2014), layered complexes (Lenaz et al., 2007; 2011; 2012), Alpine peridotites (Basso et al., 1984; Lenaz et al., 2010), komatiites (Lenaz et al., 2004), kimberlites and chromites included in diamonds (Lenaz et al., 2009). When looking at the distribution of ophiolitic chromite on the basis of structural parameters, two groups may be identified: the first group is represented by chromite samples with an inverse relation *u* vs. a (Trend 1 in Figure 3), the second by samples with clear deviation from Trend 1 and a large variation of *u* values approximately defining a sub-vertical relation between *u* and a (Trend 2 in Figure 3). Notably, samples of the first group are stoichiometric (Derbyshire et al., 2013; Lenaz et al., 2014b) and follow Trend 1, whereas samples of the second group are non-stoichiometric (Bosi et al. 2004; Lenaz et al., 2014b) and follow Trend 2. The Indian chromite samples studied here fall into the second group, overlapped to oxidised chromite samples from Oman and Albania (Figure 3).

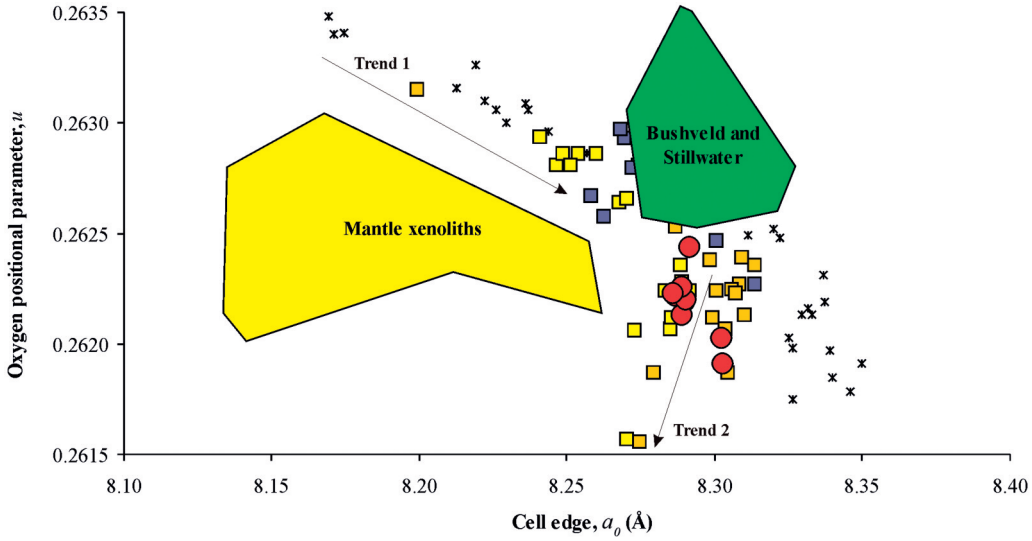

Figure 3. Oxygen positional parameter, *u*, vs. cell edge, a. Red circle = this study; orange square = Albania ophiolite (Bosi et al., 2004); purple square = Shetland ophiolite (Derbyshire et al., 2013); yellow square = Oman ophiolite (Lenaz et al., 2014b); asterisks = Alpine peridotites (Basso et al., 1984; Lenaz et al., 2010), Rum layered complex (Lenaz et al., 2011), komatiites (Lenaz et al., 2004), kimberlites and chromite included in diamond (Lenaz et al., 2009). Mantle xenoliths field includes spinels by Della Giusta et al. (1989), Princivalle et al. (1989), Carraro (2003), Uchida et al. (2005), Nédli et al. (2008), Lenaz et al. (2014a), Perinelli et al. (2014). Bushveld and Stillwater field includes spinels by Lenaz et al. (2007, 2012).

Cation distribution of the Indian chromite samples shows that Mg and Al are almost completely distributed in an ordered configuration, i.e., with Mg in T site and Al in M site. Far from being an exclusive indication of low-temperature equilibration, as occurring for Mg-Al spinels, such a distribution is almost certainly influenced by the high Cr content, which is known to hamper Mg↔Al exchange within the two sites (Lenaz et al., 2004).

The evaluation of Fe^{2+} and Fe^{3+} contents as well as site distribution will be discussed in detail for sample RN31, from the Indus Suture Ophiolite massive chromitite bands, and for sample N21, from the Indo-Myanmar Ophiolite chromitite pods. The Fe^{3+}/Fe_{tot} ratios measured by MS are 33% for RN31 and 25% for N21 (Table 3). However, the ratios calculated by EPMA data on the basis of spinel stoichiometry were quite different, being 19% for the sample RN31, and 12% (on average) for the sample N21 (Figure 4). The difference between measured and calculated Fe^{3+} contents (that is excess Fe^{3+}, ΔFe^{3+}) reaches the maximum value for sample RN31 (ΔFe^{3+} = 0.050 apfu), but is also significant for sample N21 (ΔFe^{3+} = 0.040 apfu). Both values are well beyond the experimental uncertainty (corresponding to 0.005 Fe^{3+} apfu). Accordingly, to take up this ΔFe^{3+} revealed by MS, chemical formulas need cation vacancies to

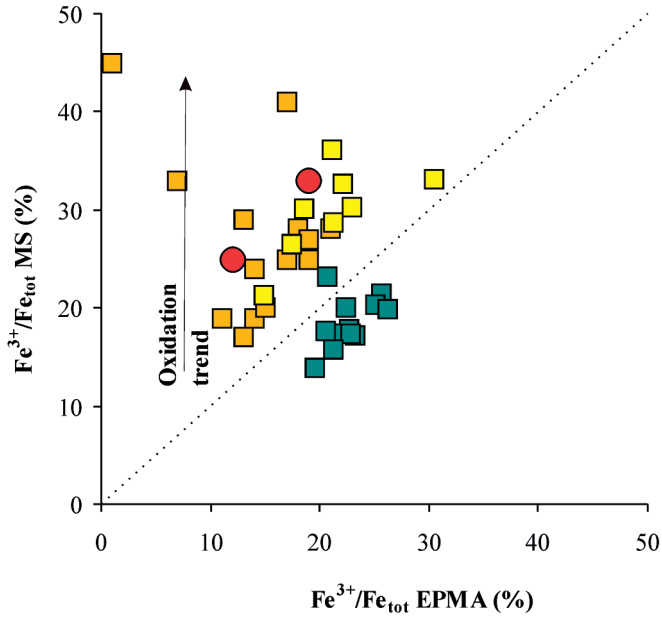

Figure 4. Comparison between Fe^{3+}/Fe_{tot} MS vs. Fe^{3+}/Fe_{tot} EPMA for different spinel occurrences. Red circle: this study; orange square: Albania ophiolite (Bosi et al., 2004); yellow square: Oman ophiolite (Lenaz et al., 2014b); green square: Bushveld layered complex (Adetunji et al., 2013).

charge-balance, estimated at 0.019 per formula unit (pfu) for sample RN31 and in the range 0.001-0.015 pfu for sample N21 (Table 4). These crystals are therefore proved to be non-stoichiometric, a common feature in both naturally and artificially oxidised spinels (Figueiras and Waerenborgh, 1997; Menegazzo et al., 1997; Carbonin et al., 1999; Bosi et al., 2004; Lenaz et al., 2014b; Perinelli et al., 2014). The amount of vacancies is also related to the oxygen positional parameter, as already reported by Bosi et al. (2004) studying chromite samples with various oxidation degree from Albania. This relation can be expressed by a 2nd order polynomial and is shown in Figure 5, where variously oxidised chromite samples from Oman ophiolites (Lenaz et al. 2014b) are also plotted. The two Indian chromite samples studied here fall within the poorly oxidised samples from Albania.

The difficulty in determining the accurate amount of vacancies in spinels, as observed for sample N21, is due to the intrinsic differences between Mössbauer and SREF approaches. This point was clarified by Lenaz et al., (2013) by comparing results of SREF, EPMA, point-MS and powder-MS collected on several chromite samples. They showed that in some cases there was a large discrepancy between SREF and powder-MS because absorbers commonly

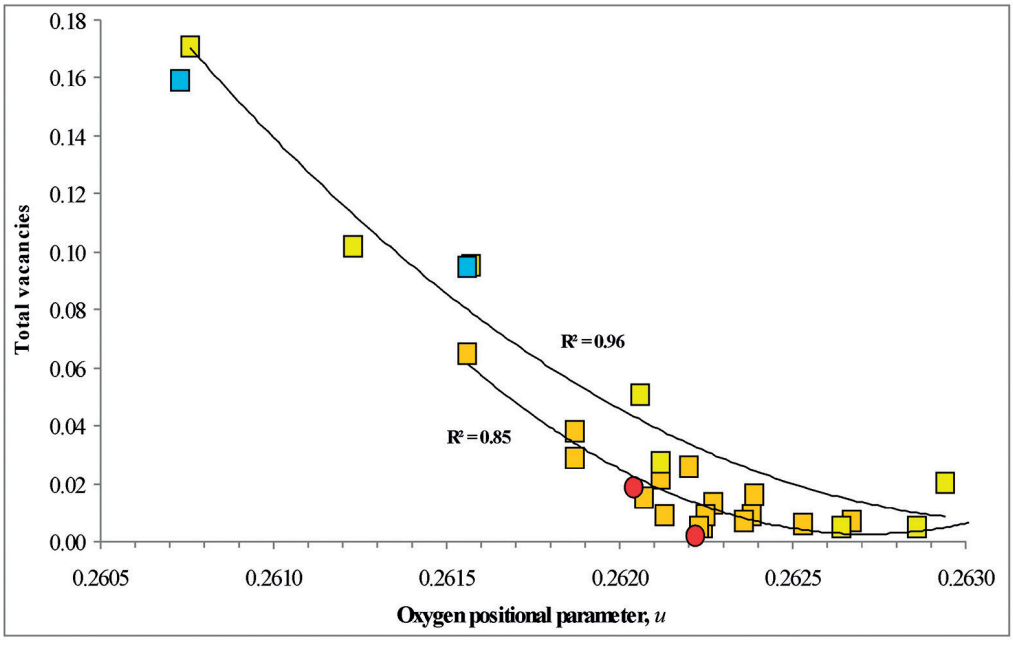

Figure 5. Total vacancies vs. oxygen positional parameter, *u*. Red circle: this study; orange square: Albania ophiolite (Bosi et al., 2004); yellow square: Oman ophiolite (Lenaz et al., 2014b); blue square: detrital Cr-spinels in terra rossa soils (Carbonin et al., 1999).

investigated by powder-MS are prepared milling a lot of grains, each of which may have very different oxidation degree, whereas SREF and point-MS are performed on the same single crystal yielding a good comparison. However, when point-MS is not available the conventional powder-MS is still the best way to evaluate the oxidation degree.

For the studied Indian chromite samples it is believed that the oxidation process (with concomitant vacancy formation) took place after primary chromite formation, probably due to an increased oxygen fugacity during a subsequent metamorphic event. In this view, it is possible to distinguish Fe^{2+} and Fe^{3+} of primary mineral formation (*P*) from those of subsequent, secondary oxidation (*S*). Under the hypothesis that primary chromite was stoichiometric, quantities calculated from EPMA will correspond to Fe^{2+}_P and Fe^{3+}_P. During the oxidation process, Fe^{3+}_S is produced (by consuming Fe^{2+}_P) and is added to Fe^{3+}_P. The above mentioned ΔFe^{3+} corresponds to Fe^{3+}_S and can be thought as equal to ($Fe^{3+}_{MS} - Fe^{3+}_P$). Following the procedure described in Menegazzo et al. (1997) and in Bosi et al. (2004), we used crystal chemical data to calculate the oxidation degree *z* (%). The parameter *z* ranges from zero (no oxidation, absence of Fe^{3+}_S) to 100% (full oxidation, all Fe^{2+}_P is oxidized to Fe^{3+}_S), and because of this it may be conveniently used to reconstruct the oxidation history of spinel samples and their host rocks. In our case, $z = 17\%$ and $z = 13\%$ were obtained for samples RN31 and N21, respectively, suggesting that the oxidation process in the two hosting chromitite assemblages was not very strong or not lasting very long time. Unfortunately, values obtained may be hardly interpreted in terms of differential cooling and possible post-magmatic processes of the two hosting assemblages, because the observed difference of oxidation degree corresponds to about twice the uncertainty associated with the process of its estimation. However, although the oxidation degree of only two chromite samples from the Indian ophiolitic belt was calculated, results obtained differ significantly from those obtained on chromite samples coming from the Nuggihalli schist belt, in the Dharwar craton of South India (Lenaz et al., 2004). In this latter case no oxidation was observed and a completely different thermo-oxidative history of the host rock can be hypothesized.

Conclusions and implications

The combined SREF-EPMA-MS approach has revealed to be particularly effective in carefully characterizing Indian ophiolitic chromites and unravelling their non-stoichiometry. This is the essential basis for a correct comparison of samples coming from different sources, either from similar petrogenetic environment or not. Coupled with the analogous results reported for ophiolitic chromites from Albania (Bosi et al., 2004), mantle xenoliths from Antarctica (Perinelli et al., 2014) and the MS results for samples in layered intrusions (Rollinson et al., 2012; Adetunji et al., 2013; Rollinson and Adetunji, 2013a,b), these findings suggest that spinel non-stoichiometry is more common than usually believed. Being the result of thermo-oxidative history of host rocks, it may be used to help reconstructing such a complex history.

Moreover, it is not restricted only to ophiolitic environment but may involve many different geological settings. The proposed multi-analytical approach is, therefore, fundamental for an accurate crystal chemical characterization of spinel (and other ferromagnesian mineral phases). This is particularly relevant when geothermobarometric calculations are performed to obtain inter- or intra-crystalline temperatures and oxygen fugacities.

Acknowledgements

The Italian C.N.R. financed the installation and maintenance of the microprobe laboratory in Padova. L. Furlan, R. Carampin and L. Tauro are kindly acknowledged for technical support. Authors would like to thank the PRIN 2010-11 fund (SPIN GEO TECH). Maibam Bidyananda gratefully acknowledges the financial support of CSIR (New Delhi) in the form of a research project. Thanks to Dr. R. Islam for the Ladakh chromitite samples. Henrik Skogby and Jorge Figueiras are kindly acknowledged for their suggestions that improved the manuscript.

References

Adetunji J., Everitt S. and Rollinson H. (2013) - New Mössbauer measurements of $Fe^{3+}/\Sigma Fe$ ratios in chromites from the early Proterozoic Bushveld Compex, South Africa. *Precambrian Research*, 228, 194-205.

Barnes S.J. (2000) - Chromite in komatiites, II. Modification during greenschist to mid-amphibolite facies metamorphism. *Journal of Petrology*, 41, 387-409.

Basso R., Comin-Chiaramonti P., Della Giusta A. and Flora O. (1984) - Crystal chemistry of four Mg-Fe-Al-Cr spinels from the Balmuccia peridotite (Western Italian Alps). *Neues Jahrbuch für Mineralogie Abhandlungen*, 150, 1-10.

Biagioni C. and Pasero M. (2014) - The systematics of the spinel-type minerals: An overview. *American Mineralogist*, in print, DOI 10.2138/am.2014.4816.

Bosi F., Andreozzi G.B., Ferrini V. and Lucchesi S. (2004) - Behavior of cation vacancy in kenotetrahedral Cr-spinels from Albanian eastern belt ophiolites. *American Mineralogist*, 89, 1367-1373.

Burkhard D.J.M. (1993) - Accessory chrome spinels: their co-existence and alteration in serpentinites. *Geochimica et Cosmochimica Acta*, 57, 1297-1306.

Carbonin S., Menegazzo G., Lenaz D. and Princivalle F. (1999) - Crystal chemistry of two detrital Cr-spinels with unusual low values of oxygen positional parameter: Oxidation mechanism and possible clues to their origin. *Neues Jahrbuch für Mineralogie Monatshefte*, 8, 359-371.

Carbonin S., Russo U. and Della Giusta A. (1996) - Cation distribution in some natural spinels from X-ray diffraction and Mössbauer spectroscopy. *Mineralogical Magazine*, 60, 355-368.

Carraro A. (2003) - Crystal chemistry of Cr-spinels from a suite of spinel peridotite mantle xenoliths from the Predazzo Area (Dolomites, Northern Italy). *European Journal of Mineralogy*, 15, 681-688.

De Grave E. and Van Alboom A. (1991) - Evaluation of ferrous and ferric Mössbauer fractions. *Physics and Chemistry of Minerals*, 18, 337-342.

Della Giusta A., Princivalle F. and Carbonin S. (1986) - Crystal chemistry of a suite of natural Cr-bearing spinels with $0.15 < Cr < 1.07$. *Neues Jahrbuch für Mineralogie Abhandlungen*, 155, 319-330.

Della Giusta A., Carbonin S. and Ottonello G. (1996) - Temperature-dependent disorder in a natural Mg - Al - Fe^{2+} - Fe^{3+} - spinel. *Mineralogical Magazine*, 60, 603-616.

Derbyshire E.J., O'Driscoll B., Lenaz D., Gertisser R. and Kronz A. (2013) - Compositionally heterogeneous podiform chromitite in the Shetland Ophiolite Complex (Scotland): Implications for chromitite petrogenesis and late-stage alteration in the upper mantle portion of a supra-subduction zone ophiolite. *Lithos*, 162-163, 279-300.

Evans B.W. and Frost B.R. (1975) - Chrome spinel in progressive metamorphism - a preliminary analysis. *Geochimica et Cosmochimica Acta*, 39, 959-972.

Figueiras J. and Waerenborgh J.C. (1997) - Fully oxidized chromite in the Serra Alta (South Portugal)

quartzites: chemical and structural characterization and geological implications. *Mineralogical Magazine*, 61, 627-638.

Hålenius U., Skogby H. and Andreozzi G.B. (2002) - Influence of cation distribution on the optical absorption spectra of Fe^{3+}-bearing spinel s.s.-hercynite crystals : evidence for electron transitions in $^{VI}Fe^{2+}$-$^{VI}Fe^{3+}$ clusters. *Physics and Chemistry of Minerals*, 29, 319-330.

Kimball K.L. (1990) - Effects of hydrothermal alteration on the compositions of chromian spinels. *Contributions to Mineralogy and Petrology*, 105, 337-346.

Lagarec K. and Rancourt D.G. (1998) - RECOIL. Mössbauer spectral analysis software for Windows, version 1.0. Department of Physics, University of Ottawa, Canada

Lavina B., Salviulo G. and Della Giusta A. (2002) - Cation distribution and structure modeling of spinel solid solutions. *Physics and Chemistry of Minerals*, 29, 10-18.

Lenaz D., Carbonin S., Gregoric M. and Princivalle F. (2002) - Crystal chemistry and oxidation state of one euhedral Cr-spinel crystal enclosed in a bauxite layer (Trieste Karst: NE Italy): Some considerations on its depositional history and provenance. *Neues Jahrbuch für Mineralogie Monatshefte*, 5, 193-206.

Lenaz D., Andreozzi G.B., Mitra S., Bidyananda M. and Princivalle F. (2004) - Crystal chemical and ^{57}Fe Mössbauer study of chromite from the Nuggihalli schist belt (India). *Mineralogy and Petrology*, 80, 45-57.

Lenaz D., Braidotti R., Princivalle F., Garuti G. and Zaccarini F. (2007) - Crystal chemistry and structural refinement of chromites from different chromitite layers and xenoliths of the Bushveld Complex. *European Journal of Mineralogy*, 19, 599-609.

Lenaz D., Logvinova A.M., Princivalle F. and Sobolev N.V. (2009) - Structural parameters of chromite included in diamonds and kimberlites from Siberia: a new tool for discriminating ultramafic source. *American Mineralogist*, 94, 1067-1070.

Lenaz D., De Min A., Garuti G., Zaccarini F. and Princivalle F. (2010) - Crystal chemistry of Cr-spinels from the lherzolite mantle peridotite of Ronda (Spain). *American Mineralogist*, 95, 1323-1328.

Lenaz D., O'Driscoll B. and Princivalle F. (2011) - Petrogenesis of the anorthosite-chromitite association: crystal-chemical and petrological insights from the Rum Layered Suite, NW Scotland. *Contributions to Mineralogy and Petrology*, 162, 1201-1213.

Lenaz D., Garuti G., Zaccarini F., Cooper R.W. and Princivalle F. (2012) - The Stillwater Complex chromitites: the response of chromite crystal chemistry to magma injection. *Geologica Acta*, 10, 33-41.

Lenaz D., Skogby H., Logvinova A.M., Sobolev N.V. and Princivalle F. (2013) - A micro-Mössbauer study of chromites included in diamond and other mantle-related rocks. *Physics and Chemistry of Minerals*, 40, 671-679.

Lenaz D., Youbi N., De Min A., Boumehdi M.A. and Ben Abbou M. (2014a) - Low intra-crystalline closure temperatures of Cr-bearing spinels from the mantle xenoliths of the Middle Atlas Neogene-Quaternary Volcanic Field (Morocco): A mineralogical evidence of a cooler mantle beneath the West African Craton. *American Mineralogist*, 99, 267-275.

Lenaz D., Adetunji J. and Rollinson H. (2014b) - Determination of $Fe^{3+}/\Sigma Fe$ ratios in chrome spinels using a combined Mössbauer and single-crystal X-ray approach: application to chromitites from the mantle section of the Oman ophiolite. *Contributions to Mineralogy and Petrology*, 167, article 958.

Li Z., Ping J.Y., Jin M.Z. and Liu M.L. (2002) - Distribution of Fe^{2+} and Fe^{3+} and next-nearest neighbour effects in natural chromites: comparison between results of QSD and Lorentzian doublet analysis. *Physics and Chemistry of Minerals*, 29, 485-494.

Menegazzo G. and Carbonin S. (1998) - Oxidation mechanism in Al-Mg-Fe spinels. A second stage: α-Fe_2O_3 exsolution. *Physics and Chemistry of Minerals*, 25, 541-547.

Menegazzo G., Carbonin S. and Della Giusta A. (1997) - Cation and vacancy distibution in an artificially oxidized natural spinel. *Mineralogical Magazine*, 61, 411-421.

Mitra S., Pal T. and Pal T.N. (1991a) - Electron localisation at B-site: a concomitant process for oxidation of Cr-spinels to a partly inverse form. *Solid State Communications*, 77, 297-301.

Mitra S., Pal T. and Pal T.N. (1991b) - Petrogenetic implication of the Mössbauer hyperfine parameters of Fe^{3+}-chromites from Sukinda (India) ultramafites. *Mineralogical Magazine*, 55, 535-542.

Miura M., Arai S., Ahmed A.H., Mizukami T., Okuno M. and Yamamoto S. (2012) Podiform chromitite classification revisited: A comparison of discordant

and concordant chromitite pods from Wadi Hilti, northern Oman ophiolite. *Journal of Asian Earth Sciences*, 59, 52-61.

Nédli Zs., Princivalle F., Lenaz D. and Tóth, T.M. (2008) - Crystal chemistry of clinopyroxene and spinel from mantle xenoliths hosted in Late Mesozoic lamprophyres (Villány Mts, S Hungary). *Neues Jahrbuch für Mineralogie Abhandlungen*, 185, 1-10.

North A.C.T., Phillips D.C. and Scott-Mattews F. (1968) - A semi-empirical method of absorption correction. *Acta Crystallographica*, A24, 351-352.

Perinelli C., Bosi F., Andreozzi G.B., Conte A.M. and Armienti P. (2014) - Geothermometric study of Cr-spinels of peridotite mantle xenoliths from Northern Victoria Land (Antarctica). *American Mineralogist*, 99, 839-846.

Prasad, U. (1984) - Petrology of Indian ophiolites. *Special Publication Geological Survey of India*, 12, 297-308.

Prince E. (2004) - International Tables for X-ray Crystallography. Volume C: Mathematical, Physical and Chemical Tables, 3rd ed. Springer, Dordrecht, The Netherlands.

Princivalle F., Della Giusta A. and Carbonin S. (1989) - Comparative crystal chemistry of spinels from some suites of ultramafic rocks. *Mineralogy and Petrology*, 40, 117-126.

Princivalle F., De Min A., Lenaz D., Scarbolo M. and Zanetti A. (2014) - Ultramafic xenoliths from Damaping (Hannuoba region, NE-China): petrogenetic implications from crystal chemistry of pyroxenes, olivine and Cr-spinel and trace element content of clinopyroxene. *Lithos*, 188, 3-14.

Quintiliani M. (2005) - ^{57}Fe Mössbauer spectroscopy analysis of spinels: Fe^{3+}/Fe_{tot} quantification accuracy and consequences on f_{O2} estimate. *Periodico di Mineralogia*, 74, 139-146.

Quintiliani M., Andreozzi G.B. and Graziani G. (2006) - Fe^{2+} and Fe^{3+} quantification of different approaches and f_{O2} estimation for Albanian Cr-spinels. *American Mineralogist*, 91, 907-916.

Rollinson H. and Adetunji J. (2013a) - Mantle podiform chromitites do not form beneath mid-ocean ridges: a case study from the Moho transition zone of the Oman ophiolite. *Lithos*, 177, 314-327.

Rollinson H. and Adetunji J. (2013b) - The geochemistry and oxidation state of podifrom chromitites from the mantle section of the Oman ophiolite: A review. *Gondwana Research*, in print, DOI 10.1016/j.gr.2013.07.013.

Rollinson H., Adetunji J., Yousif A.A. and Gismelseed A.M. (2012) - New Mössbauer measurements of $Fe^{3+}/\Sigma Fe$ in chromites from the mantle section of the Oman ophiolites: evidence for the oxidation of the sub-oceanic mantle. *Mineralogical Magazine*, 76, 579-596.

Sengupta S., Acharyya S.K., Van den Hul H.J. and Chattopadhyay B. (1989) - Geochemistry of volcanic rocks from the Naga Hills ophiolites, northeastern India and their inferred tectonic setting. *Journal Geological Society of London*, 146, 491-498.

Sengupta S., Ray K.K., Acharyya S.K. and de Smeth J.B. (1990) - Nature of ophiolite occurrences along the eastern margin of the Indian plate and their tectonic significance. *Geology*, 18, 439-442.

Sheldrick G.M. (2008) - A short history of SHELX. *Acta Crystallographica*, A64, 112-122.

Thakur V.C. (1981) - Regional framework and geodynamic evolution of the Indus Tsangpo suture zone in the Ladakh, northwest Himalaya. *Transactions of the Royal Society of Edinburgh, Earth Science*, 72, 89-97.

Tokonami M. (1965) - Atomic scattering factor for O^{-2}. *Acta Crystallographica*, 19, 486.

Uchida H., Lavina B., Downes R.T. and Chesley J. (2005) - Single-crystal X-ray diffraction of spinels from the San Carlos Volcanic Field, Arizona: Spinel as a geothermometer. *American Mineralogist*, 90, 1900-1908.

Ulmer G.C. (1974) - Alteration of chromite during serpentinization in the Pennsylvania-Maryland district. *American Mineralogist*, 59, 1236-1241.

Submitted, May 2014 - Accepted, August 2014